Journal of proteome research

Article

pubs.acs.org/jpr

Newborn Urinary Metabolic Signatures of Prematurity and Other Disorders: A Case Control Study

Joana Pinto,[†] Sílvia O. Diaz,[†] António S. Barros,[‡] Elisabete Morais,[†] Daniela Duarte,[†] Fátima Negrão,[∥] Cristina Pita,[∥] Maria do Céu Almeida,[∥] Isabel M. Carreira,[§] Manfred Spraul,[⊥] and Ana M. Gil*[,†]

[†]CICECO, Aveiro Institute of Materials, Department of Chemistry, University of Aveiro, 3810-193 Aveiro, Portugal

[‡]QOPNA Research Unit, Department of Chemistry, Campus Universitário de Santiago, University of Aveiro, 3810-193 Aveiro, Portugal

[§]Cytogenetics and Genomics Laboratory, Faculty of Medicine, University of Coimbra, Portugal and CIMAGO Center for Research in Environment, Genetics and Oncobiology, 3000, Coimbra, Portugal

[∥]Maternidade Bissaya Barreto, Centro Hospitalar e Universitário de Coimbra, CHUC, 3000 Coimbra, Portugal

[⊥]Bruker BioSpin, Silberstreifen, D-76287 Rheinstetten, Germany

Supporting Information

ABSTRACT: This work assesses the urinary metabolite signature of prematurity in newborns by nuclear magnetic resonance (NMR) spectroscopy, while establishing the role of possible confounders and signature specificity, through comparison to other disorders. Gender and delivery mode are shown to impact importantly on newborn urine composition, their analysis pointing out at specific metabolite variations requiring consideration in unmatched subject groups. Premature newborns are, however, characterized by a stronger signature of varying metabolites, suggestive of disturbances in nucleotide metabolism, lung surfactants biosynthesis and renal function, along with enhancement of tricarboxylic acid (TCA) cycle activity, fatty acids oxidation, and oxidative stress. Comparison with other abnormal conditions (respiratory depression episode, large for gestational age, malformations, jaundice and premature rupture of membranes) reveals that such signature seems to be largely specific of preterm newborns, showing that NMR metabolomics can retrieve particular disorder effects, as well as general stress effects. These results provide valuable novel information on the metabolic impact of prematurity, contributing to the better understanding of its effects on the newborn's state of health.

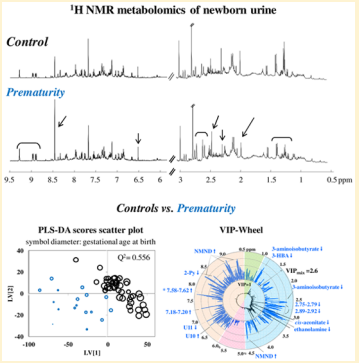

KEYWORDS: *urine, newborn, prematurity, respiratory depression, large for gestational age, malformations, metabolomics, NMR*

INTRODUCTION

Metabolomics is an exquisite tool used to measure the metabolic adaptations of the human organism to disease and seek valid metabolite signatures, potentially translatable into disease biomarkers. In newborn health research, metabolomic studies have involved nuclear magnetic resonance (NMR) spectroscopy (μM-mM detection limit) and mass spectrometry (MS) (<pM detection limit) of umbilical cord blood collected at the time of birth, newborn dried blood spots and urine, as reviewed recently,[1,2] along with a recent study of meconium in relation to newborn urine.[3] These studies have attempted to measure the metabolic effects associated with several newborn conditions, in order to define new metabolic biomarkers, which may be included in improved health management schemes for newborns. Analysis of umbilical cord blood provides a snapshot of maternal-fetal symbiosis, and compositional changes have been detected in relation to (1) perturbations in fetal growth, namely small for gestational age (SGA),[4] intrauterine growth restriction (IUGR),[5,6] low birth weight (LBW),[7] and very low birth weight (VLBW);[8] (2) hypoxic ischemic encephalopathy (HIE) and asphyxia;[9−11] (3) gestational diabetes mellitus (GDM) pregnancies[3,12]) delivery mode (vaginal delivery vs cesarean section).[13] In addition, newborn blood spots collected during the first week of life and analyzed by ^{1}H NMR and nanospray ionization with high resolution mass spectrometry (nS-HR-MS) have been studied for the screening of inborn errors of metabolism (IEM).[14−16] The noninvasive collection of newborn urine and subsequent ease to address large cohorts, compared to newborn blood, makes it a particularly interesting biofluid in the present context. This has indeed been recognized in reports on the newborn urinary impact of prematurity,[17−20] IUGR,[21−23] large for gestational age (LGA),[22,23] GDM,[3] asphyxia,[11,24,25] respiratory distress syndrome (RDS),[24] meconium aspiration syndrome (MAS),[24] bronchopulmonary dysplasia,[26] IEM,[27] neonatal sepsis,[28] postnatal bacterial,[19] cytomegalovirus,[29] and fungal[30] infections. Most of these studies have considered relatively small cohorts (up to ca. 20 disease samples), with a few studies comprising higher sample numbers.[3,20,21,25] Furthermore, specific needs

Received: October 20, 2015

DOI: 10.1021/acs.jproteome.5b00977
J. Proteome Res. XXXX, XXX, XXX−XXX

Table 1. List of Newborn Urine Samples Collected for Each Group of Healthy and Pathological Cases, Along with Corresponding Day of Life at Sampling (Days) Gestational Age Range (Gestational Weeks, g.w.), Birth Weight Range (in Kilograms, kg) and Maternal Age Range (Years) (top)[f]

Newborn disorders

Group	n			Day of life (days)	Gestational age (g.w.)	Birth weight (kg)	Maternal age (years)	Gravidity/ Parity
	Total	M/F	VD/CS					
Control	46	23/23	29/17	1-4 (2)	37-40 (39)	2.46-3.69 (3.11)	16-43 (31)	1-6(2)/ 0-3(1)
Prematurity [a,b]	17	11/6	8/9	1-6 (2)	33-36 (35)	1.26-3.28 (2.36)	23-41 (30)	1-3 (1)/ 0-2 (0)
Respiratory depression [b]	10	4/6	6/4	1-2 (2)	36-40 (39)	2.49-3.49 (3.13)	20-36 (33)	1-4 (2)/ 0-1(1)
LGA [b]	18	14/4	7/11	1-2 (2)	38-40 (39)	3.70-4.76 (3.92)	20-38 (34)	1-4 (2)/ 0-3 (1)
Malformations [b]	9	6/3	2/7	2-3 (2)	37-40 (39)	2.61-3.59 (3.02)	19-40 (33)	1-4(2) 0-3(1)
PROM	33	21/12	20/13	1-3 (2)	37-40 (39)	2.58-4.16 (3.30)	19-41 (32)	1-4 (1)/ 0-3(1)
Jaundice development	12	8/4	8/4	1-3 (2)	35-40 (38)	2.16-3.47 (2.99)	24-41 (33)	1-3 (1)/ 0-1(0)

Confounding effects investigated

Gender [c]	Delivery mode [d]	Gestational age (g.w.)	Day of life
Female n= 23	VD n= 29	37≤ GA<38 n=5	Day 1 n= 7
Male n=23	CS n= 17	38≤ GA<39 n=10	Day 2 n=31
		39≤ GA<40 n=18	Day 3 n=2
		40≤ GA<41 n=13	Day 4 n=2
			Day 1-3 [e] n=4

[a]The prematurity includes one case of SGA. [b]Conditions observed to have a large impact on newborn urinary metabolome. [c,d]Groups matched for delivery mode and gender, respectively. [e]Exact day of collection not specified. [f]Samples used for investigation of potential confounding effects are also listed (control samples only). Median values are shown between brackets. PROM: premature rupture of membranes, LGA: large for gestational age, GA: gestational age, VD: vaginal delivery, CS: cesarean section.

have been identified in order to enable the applicability of newborn metabolic biomarkers in the clinic, namely the need to adequately validate the new findings (at both statistical and biochemical levels), gauge the impact of potential confounders (e.g., gender, delivery mode, early nutrition, ethnicity) and evaluate biomarker specificity to disease. In any case, some evidence of metabolic disturbances has already been identified, namely for newborns affected by prematurity (impact on renal and liver function, neuronal development, and amino acids metabolism);[17−20] GDM (disruption of lipid, amino acid, and nucleotide metabolisms[3]); asphyxia, RDS and MAS (changes in glucose, lactate, tricarboxylic acid (TCA) cycle metabolites and organic acids[11,24,25]); and IUGR (changes in insulin secretion, protein synthesis and catabolism, lipid synthesis, and cell proliferation[31]).

In this paper, we report, for the first time to our knowledge, the effects of important possible confounders on the urine metabolome of healthy newborns, namely, gender, delivery mode (previously studied through umbilical cord blood only[13]), gestational age at birth and day-of-life at collection. Taking these effects into account, the impact of prematurity on newborn urine composition is then assessed, building up on previous studies,[17−20] and compared to several other disorders (namely respiratory depression: newborns requiring reanimation after birth; LGA: birth weight above 90th percentile; malformations; jaundice: hyperbilirrubinemia requiring phototherapy; and premature rupture of membranes (PROM): labor after 37th g.w.), in order to assess signature specificity to prematurity. To our knowledge, this is the first report to consider several newborn conditions concomitantly, to enable disease-specific changes to be identified (apart from general stress effects on the newborn), while exploiting the use of a variable selection methodology[32] to reduce NMR data sets and strengthen the predictive power of multivariate analysis models, thus aiding in the identification of relevant biomarker signatures.

EXPERIMENTAL SECTION

Samples

Newborn urine samples were collected at the Maternity Bissaya Barreto, University Hospital Center of Coimbra (CHUC), under CHUC ethical committee approval (refs.18/04 and 29/09), with parental informed consents obtained for each infant. Clinical information was obtained from obstetrical and neonatal medical records and individual questionnaires filled at the time of collection. Table 1 lists sample numbers for all groups (total n = 148) as well as corresponding day of life at sampling, gestational age at birth, birth weight, maternal age, gravidity (no. pregnancies), and parity (no. deliveries). Most subjects were breastfed, with the following exceptions: n = 4 fed with formula milk (three controls and one LGA) and n = 15 fed with a mix of maternal/formula milk (one control, six premature newborns, six LGA and two respiratory depression). The control group comprised healthy term newborns (n = 46), born from healthy mothers and normal pregnancies; for this group,

DOI: 10.1021/acs.jproteome.5b00977
J. Proteome Res. XXXX, XXX, XXX−XXX

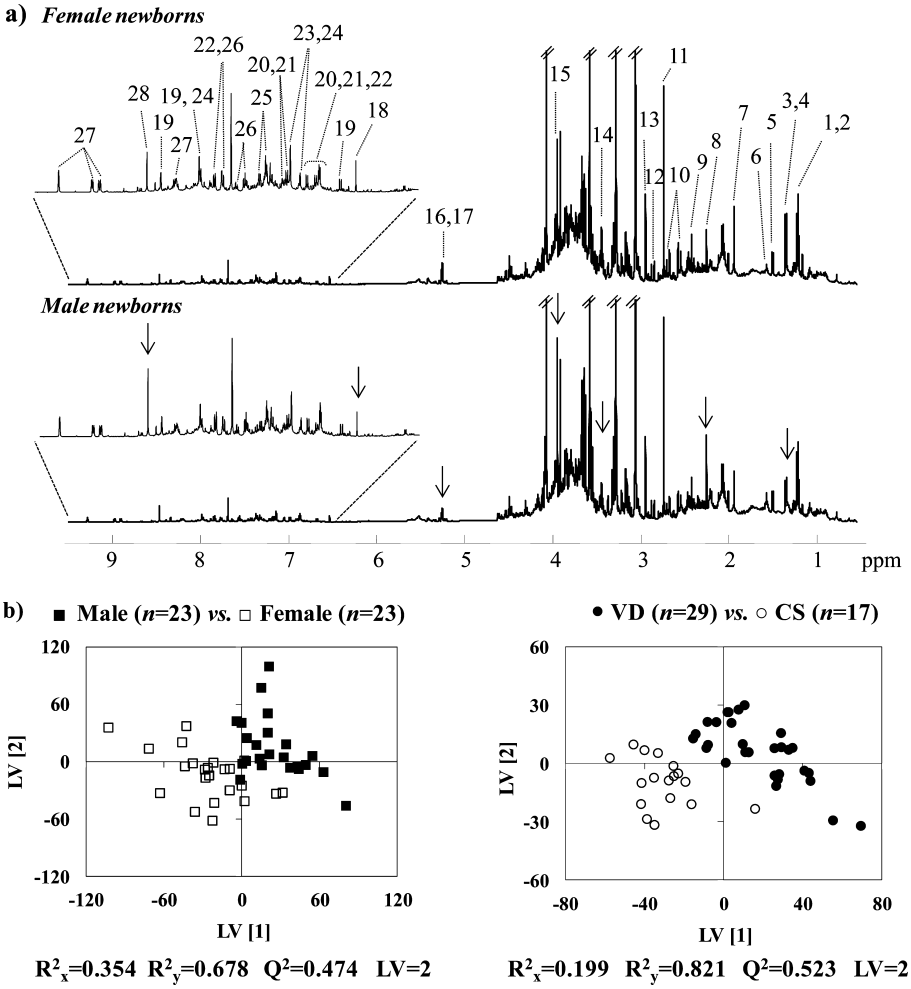

Figure 1. (a) Average 500 MHz ^{1}H NMR spectra of female and male newborns with indication of major visual changes (see arrows), (b) PLS-DA scores scatter plots obtained (with variable selection) for newborns urine in relation to gender (left): male (■, n = 23) vs female (□, n = 23), and to delivery mode (right): vaginal delivery (VD) (●, n = 29) vs cesarean section (CS) (○, n = 17). Legend: 1:3-aminoisobutyrate, 2:3-hydroxybutyrate (3-HBA), 3: lactate, 4: threonine, 5: alanine, 6: adipate, 7: acetate, 8: acetone, 9: succinate, 10: citrate, 11: dimethylamine (DMA), 12: methylguanidine, 13: dimethylglycine (DMG), 14: taurine, 15: creatine, 16: glucose, 17: lactose, 18: fumarate, 19: *N*-methyl-2-pyridone-5-carboxamide (2-Py), 20:4-hydroxyphenylacetate (4-HPA), 21: tyrosine, 22:4-hydroxyhippurate, 23:1-methylhistidine, 24: histidine, 25: phenylacetylglutamine (PAG), 26: hippurate, 27: *N*-methyl-nicotinamide (NMND), 28: formate.

the impact of gender, delivery mode (vaginal delivery (VD) or cesarean section (CS)), age (day 1 or day 2, other days not studied due to low number of samples), and gestational age at birth (37 to 41 gestational weeks, g.w.) on urine composition were investigated. Newborn urine collected for disorders included (1) late premature newborns (birth ranging from 33 to 36 g.w., n = 17), (2) newborns having experienced a respiratory depression episode after birth (newborns requiring reanimation after birth, either using oxygen or air), n = 10), (3) LGA newborns (birth weight >90th percentil, n = 18), (4) malformed newborns (n = 9 including 1 major malformation: *situs inversus* with dextrocardia, and 8 minor malformations: 5 cardiac, 2 soft tissues, and 1 urogenital), (5) PROM (labor after 37th g.w., n = 33) and (6) newborns developing jaundice 1−2 days *after* collection and requiring phototherapy, n = 12.

Urine was collected using the cotton-ball method, consisting of the placement of a sterile cotton-ball inside the newborns diaper, for up to 3 h, to retain urine (approximately 1.5 mL). Urine was transferred to a sterile vial and frozen at −20 °C for up to 24 h and then transferred to −80 °C until analysis. Samples were thawed and 600 μL were centrifuged (4500*g*, 5 min). Then, 60 μL of 1.5 M KH_2PO_4/D_2O buffer pH 7, 0.1% Na^+/3-trimethylsilyl-propionate (TSP) were added to 540 μL of supernatant, followed by pH readjustment to 7.00 ± 0.02 with KOD (4 M) and/or DCl (4 M). The mixture was centrifuged (4500*g*, 5 min) and 550 μL of the supernatant were transferred to a 5 mm NMR tube.

NMR Spectroscopy

NMR spectra were recorded on a Bruker Avance DRX 500 spectrometer at 300 K. Standard 1D spectra were acquired using a noesy 1D pulse sequence with a mixing time t_m of 100 ms, a fixed delay t1 of 3 μs, and water suppression during relaxation delay and mixing time. 128 transients were acquired into 64 k complex data points, with a 10080.65 Hz spectral width, a 4 s relaxation delay and a 3.25 s acquisition time. Each free induction decay was multiplied by a 0.3 Hz exponential line-broadening function prior to Fourier transformation. The spectra were manually phased and baseline corrected and chemical shifts referenced internally to TSP at δ = 0.0 ppm. Peak assignments were carried out with basis on literature, 2D NMR experiments (total correlation spectroscopy, TOCSY and heteronuclear single quantum coherence, HSQC), consultation

DOI: 10.1021/acs.jproteome.5b00977
J. Proteome Res. XXXX, XXX, XXX−XXX

Table 2. Metabolite/Resonance Changes in Newborn Urine of Infants Born through Vaginal Delivery (VD) Compared to Cesarean Section (CS) (Left) and Females Compared to Males (Right)

Female (n=23) *vs.* Male (n=23)			CS (n=17) *vs.* VD (n=29)		
Compound	δ_H/ppm and multiplicity [a]	Variation (effect size, p-value [b])	Compound	δ_H/ppm and multiplicity [a]	Variation (effect size, p-value [b])
2-KG [e]	2.45 t, 3.01 t	↑	1-methylhistidine [c]	7.04 s, 7.78 s	↑
4-OH-hippurate [c]	6.98d	↓	2-KG	2.45 t	↑
Acetone [d]	2.23 s	↓	4-DEA	1.11 d	↓
Allantoin [e]	5.39 s	↑ (0.81±0.60, 2.35e^{-2})	4-HPA [c]	7.17 d	↓
Cis-aconitate [e]	3.12 d	↑	Acetone	2.23 s	↑ (0.86±0.62, 5.89e^{-2})
Creatine	3.04 s	↓	Betaine	3.26 s, 3.91 s	↑
DMA [c,d]	2.72 s	↓	*Cis*-aconitate	3.12 d	↓
Formate [e]	8.46 s	↓	DMA [c]	2.72 s	↑
Fumarate [d]	6.53 s	↑	Ethanolamine	3.84 t	↑
Galactose [e]	4.59 d, 5.28 d	↓	IS	7.51 d, 7.70 d	↓ (-0.92±0.63, 1.54e^{-2})
Glucose	3.24 dd, 3.92 dd, 5.25 d	↑ (0.83±0.60, 4.89e^{-2})	Lactose	4.46 d, 5.25 d, 3.28 t. 3.55 m, 3.59 d, 3.66 m, 3.73 t, 3.79 m, 3.94 m	↑
Hippurate [c]	7.56 t, 7.64 t, 7.84	↓	*Myo*-inositol	3.55 dd	↓
Lactose [e]	5.25 d, 3.55 m, 3.59 d, 3.66 m, 3.73 t, 3.79 m, 3.94 m	↑ (0.93±0.61, 8.06e^{-2})	PAG [c]	7.36 m, 7.43 m	↓ (-0.71±0.62, 5.89e^{-2})
			Trigonelline [c]	9.12 s, 8.84 m	↓ (-0.96±0.63, 7.71e^{-2})
Lysine [e]	1.73 m	↓ (-0.71±0.60, 8.06e^{-2})	Tyrosine	6.91 d	↓
Methylguanidine [e]	2.83 s	↑	U6	0.56 s	↓ (-0.71±0.62, 8.24e^{-2})
Myo-inositol [e]	3.29 t, 3.55 dd, 3.63 t, 4.08 t	↓ (-0.86±0.60, 4.58e^{-2})	U7	2.06 s	↑ (1.04±0.64, 2.14e^{-2})
NMND	4.48 s, 8.18 m, 8.90 d, 8.97 d, 9.28 s	↑	U8	3.96 s	↑ (0.93±0.63, 5.89e^{-2})
			Unassigned spectral regions		
Scyllo-inositol [e]	3.36 s	↓ (-0.61±0.59, 4.89e^{-2})	2.90-2.92		↑ (0.80±0.62, 5.50e^{-2})
Taurine	3.43 t	↑ (0.69±0.59, 8.77e^{-2})	2.94-2.99		↑ (1.05±0.64,1.54e^{-2})
Threonine	4.26 dd	↑	3.19-3.20		↑ (0.97±0.63, 2.67e^{-2})
Xanthine*	7.93 s	↑ (1.01±0.61, 3.64e^{-2})	3.22-3.24		↑ (0.50±0.61, 8.93e^{-2})
U1	5.35 t [3.64]	↑ (0.67±0.59, 6.68e^{-2})			
U2	5.41 d [3.56, 3.78]	↑ (0.72±0.60, 2.96e^{-4})	3.97-4.01		↑ (0.75±0.62, 8.24e^{-2})
			6.71-6.74		↓ (-0.71±0.62, 8.93e^{-2})
			7.24-7.30		↓ (-0.91±0.63, 1.22e^{-2})
U3	5.45 m [2.84]	↓ (-0.72±0.60, 4.89e^{-2})	8.64-8.67		↓ (-0.80±0.62, 5.89e^{-2})
U4	5.59 d [1.61 m, 2.06, 2.96]	↓ (-0.75±0.60, 4.89e^{-2})	+ 4 Unassigned spin and 6 Regions with p>0.05		
U5	6.07 d	↓ (-0.71±0.60, 4.89e^{-2})			
Unassigned spectral regions					
1.57-1.66		↓ (-0.57±0.59, 8.59e^{-2})			
2.17-2.20		↓ (-0.65±0.59, 8.77e^{-2})			
2.80-2.82		↑ (0.54±0.59, 4.89e^{-2})			
4.32-4.34		↑ (0.74±0.60, 4.89e^{-2})			
6.11-6.12		↓ (-0.85±0.60, 4.89e^{-2})			
6.30-6.34		↓ (-0.75±0.60, 5.22e^{-2})			
6.36-6.38		↓ (-0.63±0.59, 4.89e^{-2})			
6.39-6.41		↓ (-0.84±0.60, 4.89e^{-2})			
6.46-6.49		↓ (-1.09±0.62, 2.35e^{-2})			
6.60-6.62		↓ (-0.83±0.60, 4.89e^{-2})			
8.03-8.07		↑ (0.81±0.60, 4.89e^{-2})			
+ 6 Unassigned spin and 6 Regions with p>0.05					

[a]Chemical shifts selected by variables selection; TOCSY or STOCSY correlated peaks in square brackets; s: singlet, d: doublet, t: triplet, q: quartet, dd: doublet of doublets, m: multiplet, br: broad. [b]p-values adjusted for multiple testing according to Benjamini and Hochberg false discovery rate correction[40]. [c]Peaks possibly related to diet and/or gut microflora. [d]Consistent with gender-specific changes reported in adults.[41,42] [e]Metabolites identified for the first time in connection to gender. *Putative assignment. U*i*: unassigned compound *i* in order of appearance. 2-KG: 2-ketoglutarate, DMA: dimethylamine, 4-DEA: 4-deoxyerythronic acid, 4-HPA: 4-hydroxyphenylacetate, IS: indoxyl sulfate, PAG: phenylacetylglutamine, NMND: *N*-methyl-nicotinamide. Effect size values equal or lower than error, concomitantly with p-values > 0.05, are not shown.

of spectral databases (Bruker Bbiorefcode database and human metabolome database, HMDB[33]), spectra of standard compounds and statistical total correlation spectroscopy (STOCSY).[34]

Statistical Analysis and Validation

Proton 1D spectra were aligned using a recursive segment-wise peak alignment,[35] normalized by probabilistic quotient normalization (PQN)[36] (MATLAB 7.12.0, The MathWorks Inc.) and scaled by unit variance (SIMCA-P 11.5). Principal component analysis (PCA) and partial least-squares discriminant analysis (PLS-DA) were applied to the full resolution spectra (after exclusion of water (4.62−5.05 ppm) and urea (5.65−6.00 ppm) regions) and variable selection was performed, as described previously.[32] On average, it was found through variable selection that $^1/_4$ to nearly $^1/_3$ of variables (chemical shifts) were adequate to build classification models with predictive power (Supporting Information (SI) Table S2). PLS-DA model validation was assessed for full resolution and reduced data sets, through Monte Carlo cross validation (MCCV, in-house developed) (7 blocks, 500 runs), with recovery of Q^2 values and confusion matrices; simultaneously, a randomized class-permutation procedure used to assess the null hypothesis.[37,38] Classification rates (CR), specificity (spec.) and sensitivity (sens.) were computed and model predictive power was further complemented using a receiver operating characteristic (ROC) map, a function of the true positive rate (TPR or sensitivity) and false positive rate (FPR or 1-specificity). PLS-DA models were considered satisfactorily robust when exhibiting Q^2 > 0.4, high CR, sensitivity and specificity, good quality ROC maps and true and permuted Q^2 values distributions (with >97% of permuted models with Q^2 lower than the original Q^2 value). SI Table S2 lists the model quality parameters obtained for all PLS-DA models and robust models are shown in bold. The

DOI: 10.1021/acs.jproteome.5b00977
J. Proteome Res. XXXX, XXX, XXX−XXX

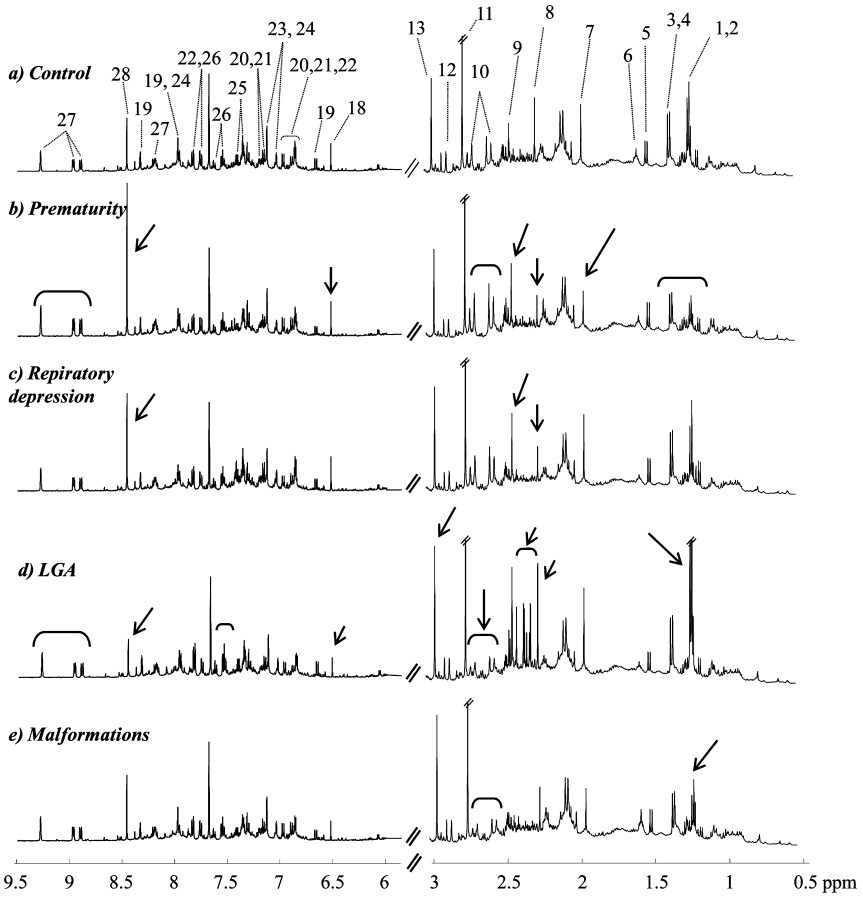

Figure 2. Average 500 MHz ^{1}H NMR aliphatic (0.5−3.0 ppm, right) and aromatic (6.0−9.5 ppm, left) regions of urine of (a) controls, (b) prematurity, (c) respiratory depression, (d) LGA, and (e) malformations newborn groups. Some relevant assignments are noted in (a), following the peak numbering defined in Figure 1a. Major visual changes are indicated with arrows and curved lines in b−e) for each disorder group.

selected variables giving rise to robust PLS-DA models were represented graphically in a variable importance to projection (VIP)-wheel format,[32] where inner and outer circles represent the average ^{1}H NMR spectrum of controls and corresponding ppm scale, respectively, and the radial dimension reflects the VIP value for each variable. The relevant peaks were integrated in the full resolution spectra (Amix 3.9.5, Bruker BioSpin, Rheinstetten, Germany) and normalized by PQN. For each integral, statistical and biological relevancies were respectively calculated by the Wilcoxon test (statistical relevance defined as $p < 0.05$) and effect size (ES).[39] ES represents the difference between the averages of two groups and is computed by $ES = (\bar{X}_1 - \bar{X}_2)/((n_1 - 1)s_1^2 + (n_2 - 1)s_2^2/(n_1 - n_2 - 2))^{1/2}$, where $\bar{X}_j$, s_j, and n_j represent the mean, standard deviation and sample size of two groups (j = 1,2), respectively. P-values were corrected for multiple comparisons using false discovery rate correction based on Benjamini and Hochberg method.[40]

RESULTS

Effects of Gender, Delivery Mode, Gestational Age, and Day of Collection

First, the impacts of gender, delivery mode, gestational age at birth and day of collection on newborn urine composition were assessed, since differences in these parameters are bound to be found in larger cohorts. The average ^{1}H NMR spectra of healthy female and male newborns (Figure 1a) illustrate the high number of peaks and peak overlap typical of urine spectra. A total of 56 metabolites were assigned (SI Table S1), including a first account, to our knowledge, of phenylacetylglutamine (PAG) and indoxyl sulfate (IS) in newborn urine. Visual inspection of the spectra in Figure 1a suggests that females' newborn urine has higher levels of fumarate (peak 18), glucose (peak 16), lactose (peak 17), taurine (peak 14), and threonine (peak 4), and lower amounts of acetone (peak 8), creatine (peak 15), and formate (peak 28) than males. PCA of the NMR spectra showed only a vague distinction between groups (not shown) and the corresponding PLS-DA model (not shown) had a relatively low predictive power (Q^2 0.270, SI Table S2). Variable selection is useful to filter off random variability (i.e., noise) in the data and therefore retrieve consistent variations related to the condition under study. Variable selection produced a new PLS-DA model for gender (Figure 1b left), with improved predictive power (Q^2 0.474, SI Table S2, Figure S1a), although of low sens., spec. and CR (75−76%). A VIP-wheel representation (SI Figure S2a) indicated allantoin, *myo*-inositol, lysine, taurine, xanthine, sugar (5.50−5.56 ppm), purine/pyrimidine resonances (6.11−6.48 ppm), and unassigned resonance at δ 7.06 as important contributors toward gender group separation. This type of representation offers a graphic description of the spectral profile variations between the groups compared. The full metabolite signature describing the changes in female urine, compared to males, is listed in Table 2 and comprises changes in several unassigned spin systems (U1−U5) and regions (complex spectral segments accommodating several overlapped resonances), with distinct

DOI: 10.1021/acs.jproteome.5b00977
J. Proteome Res. XXXX, XXX, XXX−XXX

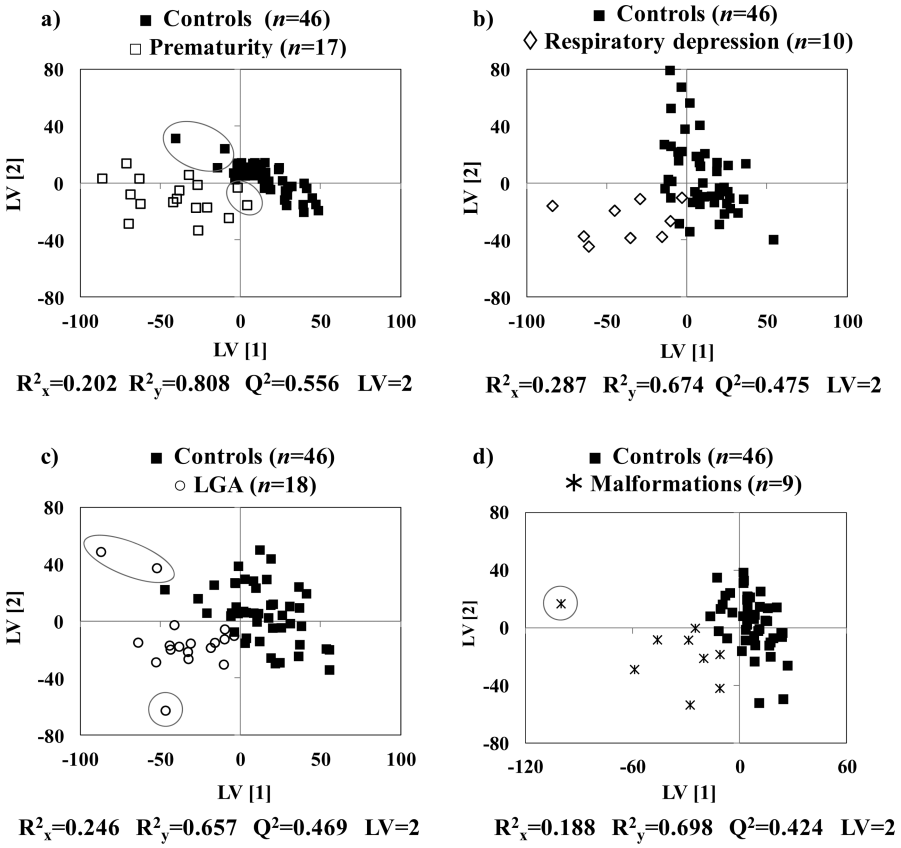

Figure 3. PLS-DA scores scatter plots obtained for (a) prematurity (□, *n* = 17), (b) newborns with respiratory depression (◇, *n* = 10), (c) LGA newborns (○, *n* = 18), and (d) malformations (∗, *n* = 9) compared to controls (■, *n* = 46). Circles indicate outlier samples.

univariate statistical relevance, as also illustrated in a Volcano plot (SI Figure S2a). Changes in acetone, dimethylamine (DMA) and fumarate coincide with earlier reports on human adults[41−44] and changes in 10 additional metabolites ([e] in Table 2, left) are here reported for the first time in connection to gender. Overall, compared to males', newborn females urine was confirmed to comprise higher levels of 2-ketoglutarate (2-KG), allantoin, *cis*-aconitate, fumarate, glucose, lactose, methylguanidine, *N*-methyl-nicotinamide (NMND), taurine, threonine, and xanthine, and lower levels of 4-OH-hippurate, acetone, creatine, DMA, formate, galactose, hippurate, lysine, *myo*-, and *scyllo*-inositols.

A similar strategy was followed to compare the impact of delivery through cesarean section and vaginal delivery. Upon variable selection, a PLS-DA model with Q^2 0.523 and 79−94% sens., spec. and CR was obtained (Figure 1b right, SI Table S2), reflecting a detectable impact of delivery mode on newborn urine composition. The corresponding VIP-wheel plot (SI Figure S2b) identified important changes in DMA, IS, tyrosine, trigonelline, unassigned singlets U7 and U8 (at δ 2.06 and 3.96, respectively) and regions (bile acids, aliphatic and aromatic resonances). Overall, variations of assigned compounds noted in CS cases, compared to VD (Table 2, right and Volcano plot in SI Figure S2b), bear increases in 1-methylhistidine, 2-KG, acetone, betaine, DMA, ethanolamine, lactose, and decreases in 4-deoxyerythronic acid (4-DEA), 4-hydroxyphenylacetate (4-HPA), *cis*-aconitate, IS, *myo*-inositol, PAG, trigonelline and tyrosine.

Regarding gestational age at birth (from 37 to 41 g.w.) and day of collection (days 1 and 2, only), no significant changes in urinary composition were noted, other aspects such as type of anesthetics at delivery and type of feeding (maternal or formula milk) not having been studied specifically, due to the low sample numbers representing each condition. The effects of gender and delivery mode described above should, thus, be considered in newborn disorder studies, particularly when control and disease groups are unbalanced in these respects.

Effects of Prematurity and Comparison with Other Newborn Disorders

Figure 2b shows the average ^{1}H NMR spectrum (aliphatic and aromatic regions) corresponding to premature newborns, with indication of apparent visual differences, compared to controls (Figure 2a). PLS-DA of variable selected matrices clearly differentiated the prematurity group from controls in LV1 (Q^2 0.556, Figure 3a), with 92% sens., spec. and CR (SI Figure S1b and Table S2). The results suggest that positive and negative LV1 values reflect normal and disturbed metabolic profiles, respectively, although a small group overlap is noted (circled symbols in Figure 3a). It is interesting to note that such separation is clearly not simply explained by gestational age or birth weight (SI Figure S3), higher values of these characteristics not translating necessarily into healthy metabolic profiles; this emphasizes the importance of using metabolic profiles as additional health assessment markers. Considering the whole prematurity group, an overall metabolic signature descriptive of the condition may be retrieved, as shown by the corresponding VIP-wheel (Figure 4a), which reflects a variation fingerprint with large contributions from 3-aminoisobutyrate, 3-hydroxybutyrate (3-HBA), *cis*-aconitate, ethanolamine, *N*-methyl-2-pyridone-5-carboxamide (2-Py) and NMND along with

DOI: 10.1021/acs.jproteome.5b00977
J. Proteome Res. XXXX, XXX, XXX−XXX

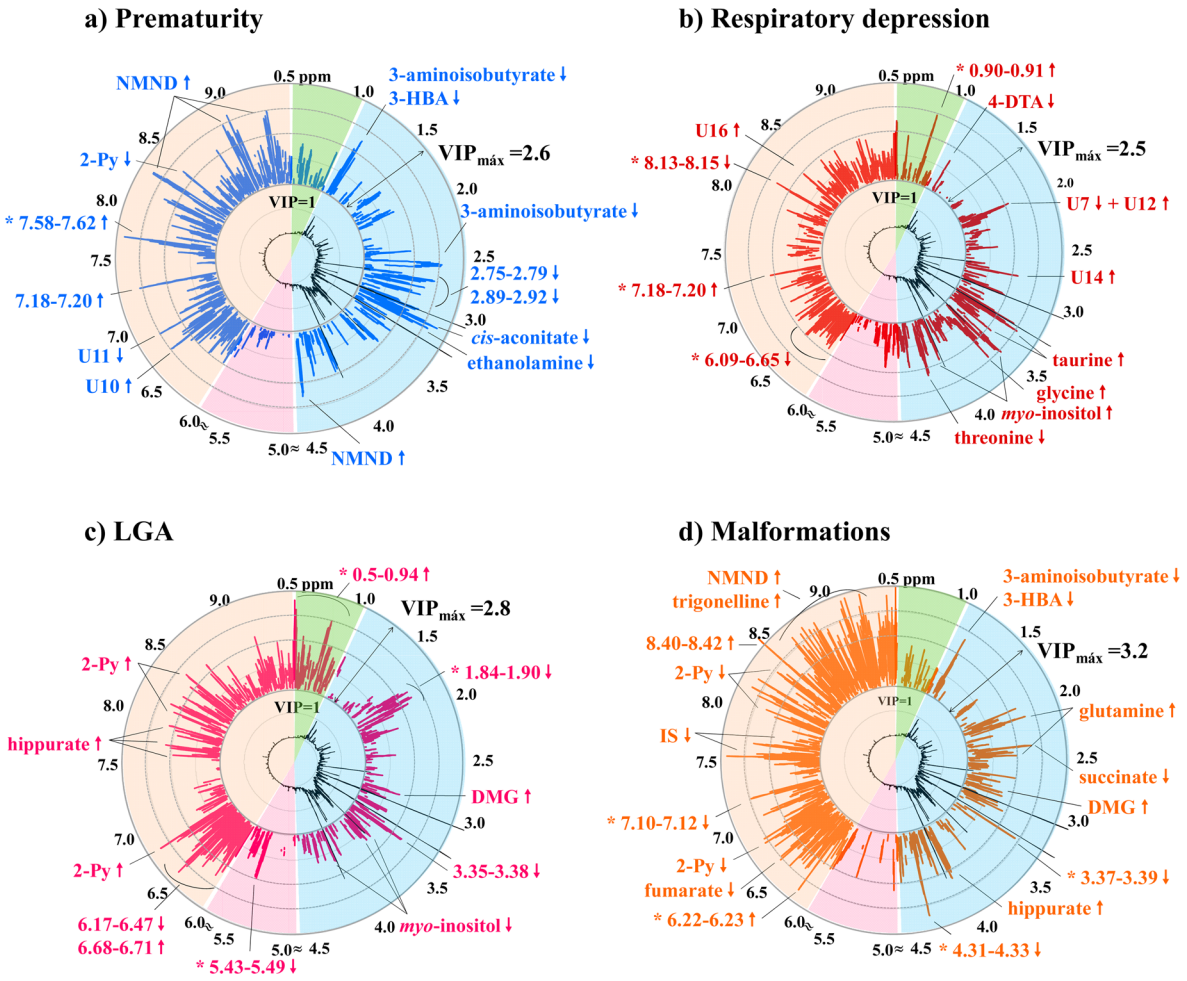

Figure 4. VIP-wheel representation of the NMR metabolite signatures obtained for (a) prematurity, (b) respiratory depression, (c) LGA newborns, and (d) malformations. The average ^{1}H NMR spectrum of controls is represented in the inner circle, with the corresponding ppm scale in the outer circle. Each dot represents a selected variable and the VIP value is shown in the radial scale. Colored shade indicates region typically containing resonances of bile acids (green), aliphatic region (blue), sugar region (pink), and aromatic region (orange). Metabolites or spectral regions with higher VIP values are noted. 3-HBA: 3-hydroxybutyrate, NMND: *N*-methyl-nicotinamide, 4-DTA: 4-deoxythreonic acid, DMG: dimethylglycine, 2-Py: *N*-methyl-2-pyridone-5-carboxamide, IS: indoxyl sulfate. ∗: spectral features corresponding to large VIP values but with no statistical relevance (*p* value >0.05).

unassigned U10 and U11 (singlet at δ 6.59 and doublet at δ 6.76, respectively), and several aliphatic and aromatic regions. The overall metabolic signature of prematurity (Table 3, top left) comprises changes in 25 identified metabolites and several additional unassigned resonances/regions, 29 of which with univariate statistical relevance (*p*-values <0.05), as illustrated on a Volcano plot format (Figure 5a). Among these, the increase in *myo*-inositol and NMND confirmed previous observations ([e] in Table 3).[18,19] Considering that the prematurity group was somewhat unbalanced in terms of gender (11*M*/6F, compared to 23*M*/23F in controls), a possible contribution of gender must be allowed for ([d] in Table 3) in relation to increased 4-OH-hippurate, formate, fumarate, lysine, *myo*-inositol, and decreased methyl-guanidine and xanthine.

In order to establish if the above signature is specific of prematurity or if, on the contrary, it reflects general stress effects on the newborn, other disorders were investigated for comparison. Indeed, spectral profile changes were also noted for newborns experiencing respiratory depression, LGA and malformations (Figure 2c–e) (no relevant changes were noted for PROM and jaundice-developing groups), but the corresponding signatures were found to be distinct from that of prematurity. Specifically, newborns suffering from respiratory depression evidenced some PLS-DA separation from controls (Figure 3b, SI Table S2) and, in spite of the low sample numbers, a VIP-wheel pattern visually distinct from prematurity was obtained (Figure 4b), thus illustrating the specificity of the two sets of metabolite changes. Respiratory depression seems to induce a distinct signature determined by 4-deoxythreonic acid (4-DTA), glycine, *myo*-inositol, taurine, threonine, U7 (s, δ 2.06), U12 (s, δ 2.05), U14 (s, δ 2.81), U16 (s, δ 8.39), along with several unassigned regions with no individual statistical relevance (∗ in Figure 4b), but important as part of a classification profile. Overall, changes in 21 identified metabolites and several unassigned resonances/regions, 17 of which characterized by individual statistical significance (p < 0.05) were found to characterize respiratory depression (Table 3, top right; Figure 5b). Regarding LGA and malformed newborns, PLS-DA performance is comparable (SI Table S2), with clear outlier samples being noted in both cases (Figure 3c,d): in LGA, the outliers contained abnormally high levels of unassigned resonance δ 0.70–1.07 (bile acid region[19]), *myo*-inositol or hippurate; in malformations, the outlier evidenced high levels of galactose. Again, the VIP-wheels (Figure 4c,d)

DOI: 10.1021/acs.jproteome.5b00977
J. Proteome Res. XXXX, XXX, XXX−XXX

Table 3. Metabolite/resonance changes in urine of preterm newborns (above left), newborn with respiratory depression (above right), LGA newborns (below left) and newborns with malformations (below right) compared to controls

Prematurity (n = 17) vs Controls (n = 46)			Respiratory Depression (n = 10) vs Controls (n = 46)		
Compound	δ_H/ppm and multiplicity[a]	Variation (effect size, p-value[b])	Compound	δ_H/ppm and multiplicity[a]	Variation (effect size, p-value)
1-methylhistidine[c]	7.78 s	↓ (-0.83 ± 0.58, $1.46e^{-2}$)	1-methylhistidine[c]	7.78 s	↓
2-Py	6.66 d, 8.33 d	↓ (-0.96 ± 0.58, $6.64e^{-3}$)	2-KG	2.45 t, 3.01 t	↓
3-aminoisobutyrate	1.19 d, 2.61 m, 3.06 dd	↓ (-1.37 ± 0.61, $3.43e^{-5}$)	3-HBA	2.31 m, 2.41 m, 4.15 m	↓
3-HBA	1.20 d	↓ (-0.49 ± 0.56, $1.46e^{-2}$)	3-methylhistidine[c]	7.15 s	↓
3-HIVA	1.27 s	↑	4-DEA	1.11 d	↓
3-methylhistidine[c]	7.15 s, 8.12 s	↓	4-DTA	1.23 d	↓
4-DTA	1.23 d	↓ (-0.61 ± 0.57, $7.84e^{-2}$)	Betaine	3.26 s, 3.91 s	↑ (1.10 ± 0.71, $7.89e^{-2}$)
4-OH-hippurate[c,d]	7.76 d	↑	Choline[c]	3.20 s	↑
Acetone	2.23 s	↓	Creatine	3.04 s, 3.93 s	↑ (0.95 ± 0.71, 7.89^{-2})
Cis-aconitate	3.12 d	↓ (-1.37 ± 0.61, $5.89e^{-5}$)	DMA	2.72 s	↓
Citrate	2.54 d, 2.69 d	↑	Formate	8.46 s	↑
Creatine	3.04 s, 3.93 s	↓	Glycine	3.57 s	↑ (1.21 ± 0.72, $6.77e^{-2}$)
Creatinine	3.05 s, 4.06 s	↓ (-0.85 ± 0.58, $2.76e^{-2}$)	Hypoxanthine	8.20 s, 8.22 s	↓
DMA[c]	2.72 s	↓ (-0.88 ± 0.58, $1.49e^{-2}$)	IS	7.70 d	↑
Ethanolamine	3.15 t, 3.84 t	↓ (-0.97 ± 0.58, $3.57e^{-3}$)	Lactose[c]	3.66 m, 3.79 m, 3.94 m, 4.46 d	↑
Formate[d]	8.46 s	↑ (0.89 ± 0.58, $1.49e^{-2}$)			
Fumarate[d]	6.53 s	↑	Lysine	1.73 m, 1.92 m	↓
IS	7.51 d	↑ (1.00 ± 0.58, $7.84e^{-2}$)	*Myo*-inositol	3.26 t, 3.55 m, 3.64 t, 4.07 t	↑ (1.54 ± 0.74, $7.89e^{-2}$)
Lactate	4.11 q	↓ (-0.76 ± 0.57, $1.72e^{-2}$)			
Lysine[d]	1.73 m	↑ (0.63 ± 0.57, $4.86e^{-2}$)	Taurine	3.43 t	↑ (0.96 ± 0.71, $7.89e^{-2}$)
Methylguanidine[d]	2.83 s	↓ (-0.78 ± 0.57, $1.46e^{-2}$)	Threonine	4.26 dd	↓
Myo-inositol[d,e]	3.26 t, 3.53 dd, 4.07 t	↑ (0.87 ± 0.58, $4.10e^{-2}$)	Trigonelline[c]	4.44 s	↓
			Xylose[c]	5.21 d	↓
NMND[e]	4.48 s, 8.90 d, 8.97 d, 9.28 s	↑ (1.20 ± 0.59, $2.94e^{-3}$)	U12	2.05 s	↑ (1.00 ± 0.71, $7.89e^{-2}$)
			U7[d]	2.06 s	↓ (-0.72 ± 0.70, $9.14e^{-2}$)
Succinate	2.41 s	↑ (0.61 ± 0.57, $7.85e^{-2}$)	U13	2.26 s	↓ (-0.82 ± 0.70, $1.14e^{-1}$)
Xanthine*[,d]	7.93 s	↓ (-0.83 ± 0.57, $8.05e^{-3}$)	U14	2.81 s	↑ (0.88 ± 0.70, $9.14\ e^{-2}$)
U9	4.51 s	↑ (0.67 ± 0.57, $1.35e^{-2}$)	U15	2.90 s [3.94 s]	↑ (0.90 ± 0.70, $7.89e^{-2}$)
U10	6.59 s	↓ (-1.24 ± 0.60, $2.70e^{-4}$)	U16	8.39 s [6.08 d]	↑ (1.10 ± 0.71, $1.18e^{-1}$)
U11	6.76 d	↓ (-1.17 ± 0.59, $7.46e^{-4}$)	**Unassigned spectral regions**		
Unassigned spectral regions			2.08–2.09		↓ (-1.00 ± 0.71, $7.89e^{-2}$)
1.99–2.01		↑ (0.73 ± 0.57, $3.59e^{-2}$)	2.10–2.12		↓ (-0.85 ± 0.70, $1.14e^{-1}$)
2.75–2.79		↓ (-1.26 ± 0.60, $8.11e^{-4}$)	2.48–2.52		↓ (-0.79 ± 0.70, $1.14e^{-1}$)
2.89–2.92		↓ (-1.06 ± 0.59, $1.51e^{-3}$)	6.61–6.62		↓ (-1.03 ± 0.71,$1.14e^{-1}$)
3.35–3.37		↑ (1.05 ± 0.59, $2.08e^{-2}$)	6.63–6.68		↓ (-1.00 ± 0.71, $1.14e^{-1}$)
7.18–7.20		↑ (1.12 ± 0.59, $1.46e^{-2}$)	+8 unassigned spin systems and 16 spectral regions with $p > 0.05$		
+ 5 unassigned spin systems and 8 spectral regions with $p > 0.05$					

LGA (n = 18) vs Controls (n = 46)			Malformations (n = 9) vs Controls (n = 46)		
Compound	δ_H/ppm and multiplicity[a]	Variation (effect size, p-value)	Compound	δ_H/ppm and multiplicity[a]	Variation (effect size, p-value)
2-KG[d]	2.45 t, 3.01 t	↓	2-Py	6.66 d, 7.97 dd, 8.33 d	↓ (-0.82 ± 0.73, $3.30e^{-1}$)
2-Py	6.66 d, 7.97 dd, 8.33 d	↑ (1.01 ± 0.57, $6.63e^{-2}$)	3-aminoisobutyrate	1.19 d, 2.61 m, 3.06 dd	↓
Alanine	1.49 d	↑			
Citrate	2.54 d, 2.69 d	↓	3-HBA	1.20 m 2.31m, 2.41 m, 4.16 m	↓
Creatine[d]	3.04 s, 3.93 s	↑			
DMG	2.93 s	↑ (0.77 ± 0.56, $5.52e^{-2}$)	4-DEA	1.11 d	↑
Fumarate[d]	6.53 s	↓	4-HPA[c,f]	6.86 d	↓
Glycine	3.57 s	↓	Acetone	2.23 s	↓
Hippurate[c,d]	3.97 d, 7.56 t, 7.64 t, 7.83 d	↑	*Cis*-aconitate[d,f]	3.12 d	↓
			Citrate	2.54 d, 2.67 d	↓
Myo-inositol	3.29 t, 3.55 t, 3.63 t, 4.08 t	↓ (-0.67 ± 0.56, $7.50e^{-2}$)	Choline[c]	3.20 s	↓
			DMG	2.93 s, 3.72 s	↑
NMND	8.18 m, 8.90 d, 8.97 d, 9.28 s	↑	Fumarate[d]	6.53 s	↓
			Glutamine	2.11 m, 2.47 m	↑
Succinate	2.41 s	↑	Hippurate[c,d]	3.97 d, 7.56 t, 7.64 t	↑
Taurine	3.43 t	↑			
Unassigned spectral regions			IS[f]	7.28 m, 7.50 d, 7.70 d	↓ (-0.78 ± 0.73, $3.30e^{-1}$)

DOI: 10.1021/acs.jproteome.5b00977
J. Proteome Res. XXXX, XXX, XXX−XXX

Table 3. continued

LGA (n = 18) vs Controls (n = 46)			Malformations (n = 9) vs Controls (n = 46)		
Compound	δ_H/ppm and multiplicity[a]	Variation (effect size, p-value)	Compound	δ_H/ppm and multiplicity[a]	Variation (effect size, p-value)
0.5−0.55		↑ (0.76 ± 0.56, 3.61e^{-2})			
0.57−0.60		↑ (0.56 ± 0.56, 4.31e^{-2})	Lactose[c,f]	3.28 t, 4.46 d	↑
0.64−0.70		↑ (0.70 ± 0.56, 7.50e^{-2})	Lysine	1.73 m	↓
0.77−0.87		↑ (0.79 ± 0.56, 1.05^{e-1})	NMND	8.90 d, 8.97 d, 9.28 s	↑
0.89−0.94		↑ (1.04 ± 0.57, 3.75e^{-2})			
3.35−3.38		↓(−0.66 ± 0.56, 7.50e^{-2})	PAG[c,f]	7.36 t, 7.43 t	↓
6.17−6.19		↓ (−0.49 ± 0.55, 7.50e^{-2})	Succinate	2.41 s	↓ (−0.95 ± 0.74, 1.68e^{-1})
			Tyrosine	6.90 d	↑
6.39−6.41		↓ (−0.65 ± 0.56, 6.01e^{-2})	Trigonelline[c]	8.84 br, 9.12 s	↑
6.43−6.45		↓ (−0.87 ± 0.57, 3.61e^{-2})	Xylose[c]	4.59 d, 5.22 d	↑
6.46−6.47		↓ (−0.80 ± 0.56, 4.69e^{-2})	U17	4.53 s [1.84 m]	↑ (0.77 ± 0.73, 3.30e^{-1})
			Unassigned spectral regions		
8.01−8.07		↑ (1.30 ± 0.59, 9.65e^{-2})	8.40−8.42		↑ (0.99 ± 0.74, 3.30e-^{1})
+ 12 unassigned spin systems and 17 spectral regions with p > 0.05			+8 unassigned spin systems and 14 spectral regions with p > 0.05		

[a, b,c,*]See Table 2 for meaning. [d]Possible contribution of gender. [e]consistent with previous prematurity studies,[18,19] [f]Possible contribution of delivery mode. U*i*: unassigned compound i by appearance order. Amino acids in 3-letter code, 2-Py: *N*-methyl-2-pyridone-5-carboxamide, DMG: dimethylglycine, *p*-CS: *p*-cresol sulfate, 3-HBA: 3-hydroxybutyrate, 3-HIVA: 3-hydroxyisovalerate, 4-DTA: 4-deoxythreonic acid, other compounds defined in Table 2. Effect size values equal or lower than error, concomitantly with p-values >0.05, are not shown.

unveiled graphically specific signatures of variations, both distinct from prematurity. LGA cases are characterized by variations in 13 metabolites, only 2-Py, dimethylglycine (DMG) and *myo*-inositol having p < 0.05) (Table 3, Figure 5c), comprising some possible contributions from gender unbalance (14*M*/4F in LGA) ([d] in Table 3). The urinary signature retrieved for the malformation group (Table 3, bottom right) comprised changes in 22 metabolites (only 2-Py, citrate, IS and succinate having p < 0.05), unassigned U17 (singlet, δ 4.53) and region at δ 8.40−8.42, with p < 0.05 (Figure 5d), with possible contributions from gender (6 M/3 F) and delivery mode (2 VD/7 CS) ([d] and [f] in Table 3, respectively). It is noted however that such signature is an average description of several types of malformations, confirming previous reports of general metabolic characteristics describing fetal malformations, as viewed by maternal urine.[32]

DISCUSSION

Figure 6 summarizes the main putative metabolic impacts on different metabolic pathways of gender and delivery mode, as well as of prematurity, respiratory depression, LGA and the heterogeneous group of malformations. Color coding by disorder helps to acknowledge both common and specific qualitative metabolic changes.

Gender and Delivery Mode

Regarding gender differences, variations in DMA, fumarate, and acetone were found to coincide (in nature and direction) with previous reports relating to adult cohorts,[41,42] while creatine, hippurate, NMND, taurine and threonine were here found to vary in opposite directions to those reported.[41−44] Other 16 metabolites reported to be gender dependent in adults were, in the present cohort, either not detected or not seen to vary. Adults and newborns seem, therefore, to be characterized by distinct gender-specific excreted metabolomes. In this cohort, the urine of females was richer in allantoin and xanthine and showed lower intensity in purines/pyrimidines region (δ 6.46−6.48), thus suggesting altered purine degradation and general nitrogen base metabolism in females, compared to males. In addition, higher levels of glucose and lactose, along with lower levels of inositols and other sugar resonances (δ 5.50−5.56), were indicative of changes in sugar metabolism associated with gender in the first days of life. *Myo*-inositol can be endogenously synthesized from glucose and is converted to *scyllo*-inositol in the gut microflora.[45] Here, this process seems to be hindered in females, resulting in a lower utilization of glucose for inositol production. As no reports were found on differences in gender-related sugar and nucleotide metabolism in adults, it is suggested that these differences may be unique to this early age. Figure 6 (light pink arrows) shows that additional smaller changes are also observed in female newborns, compared to males, in relation to creatinine biosynthesis, methionine cycle and TCA cycle. Differences found in relation to delivery mode are consistent with previous knowledge of (1) lower gut microflora colonization in caesarian section cases, (2) increased stress associated with labor, and (3) possible alterations in hepatic metabolism.[46−49] Babies born through CS have reduced bacterial content and delayed appearance of some bacterial species[46] and this may explain the decreased levels of gut-derived metabolites such as PAG and trigonelline found in CS newborn urine (Figure 6, purple arrows). Another interesting finding regards the significant increase in excreted IS in VD newborns. IS is formed in the liver from indole, a product of intestinal tryptophan breakdown, and is known to mediate oxidative stress in human umbilical vein endothelial cells.[50] The IS increase in VD cases is consistent with the process involving increased oxidative stress, as reported.[47,49] In addition, the decreasing tendency of *myo*-inositol, found here in common to umbilical cord blood of CS cases compared to VD, may also relate to labor induced stress.[13] The CS group also accommodates a significant increase in the ketone body acetone, which may be indicative of changes in hepatic fatty acids ß-oxidation and gluconeogenesis, consistently with a previous report on CS-born piglets.[48]

Prematurity and Comparison to Other Disorders

The impact of prematurity on newborn urine was found to involve disturbances in several different pathways (Figure 6, blue arrows). The changes in NMND (↑), 2-Py (↓), and 3-aminoisobutyrate (↓) indicate a general nucleotide metabolism

DOI: 10.1021/acs.jproteome.5b00977
J. Proteome Res. XXXX, XXX, XXX−XXX

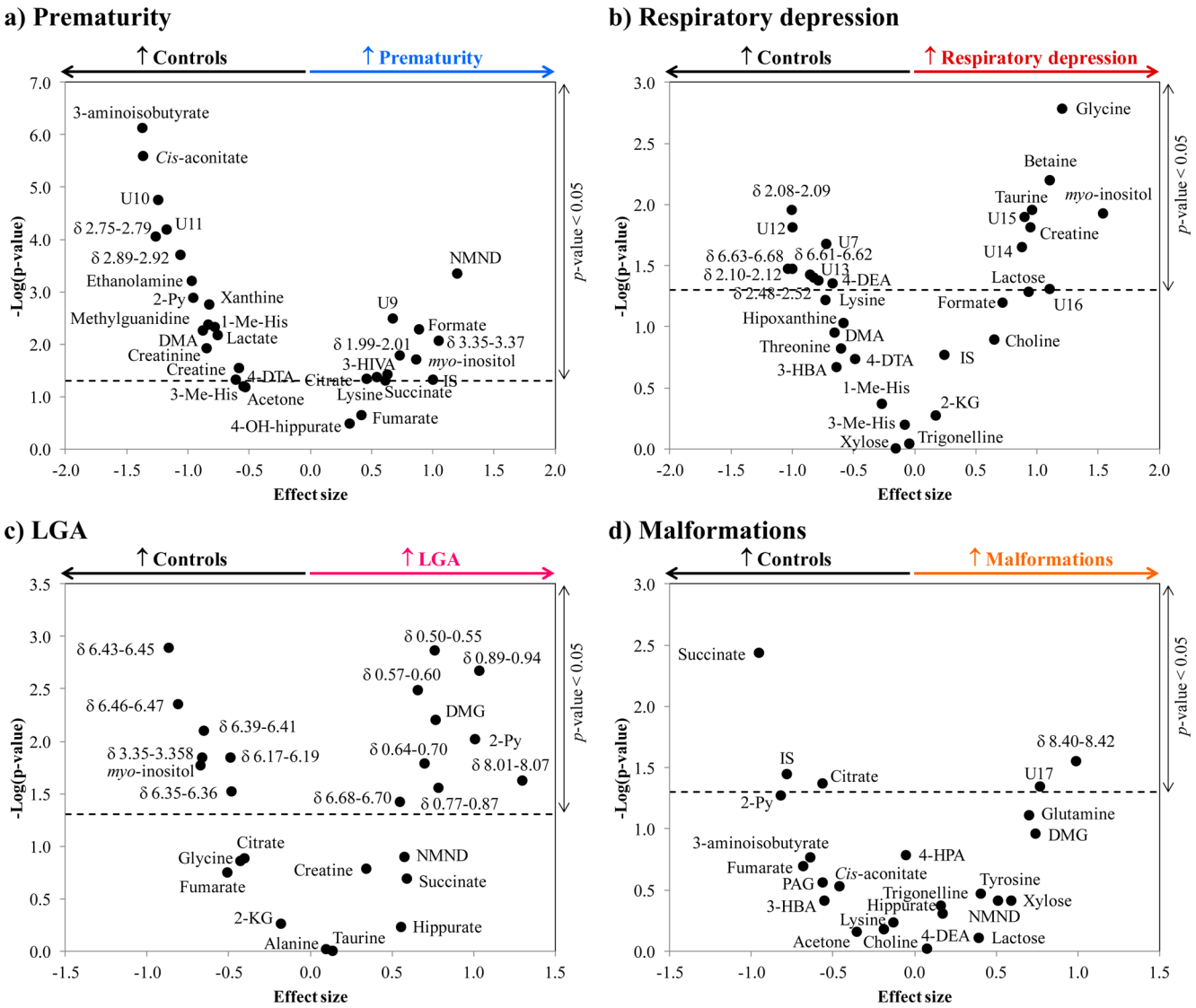

Figure 5. Volcano plots of effect size vs−log(*p*-value) of the metabolite/resonances integrals listed in Table 3 for (a) prematurity, (b) respiratory depression, (c) LGA newborns, and (d) malformations. Dashed lines indicates *p*-value = 0.05.

disturbance. NMND is formed from niacin and tryptophan to provide pyridine nucleotides to the liver and higher excreted NMND levels have been previously found in premature babies and attributed to the high concentration of tryptophan in fetal blood and its regulation after birth.[19] In this work, the increase in NMND is accompanied by a decrease in 2-Py, whereas decreased 3-aminoisobutyrate suggests a reduction in pyrimidine degradation (Figure 6). Moreover, the increase in formate may relate to its role in de novo purine biosynthesis, through activation by tetrahydrofolate (THF),[51] the suggestion of altered purines synthesis having been advanced before in studies of umbilical cord blood of premature VLBW newborns.[8] However, formate changes may also reflect gender unbalance, as well as an involvement as precursor of TCA intermediate malate. The latter possibility is consistent with the increases in citrate, fumarate and succinate, and decreased *cis*-aconitate (Figure 6), which suggest a TCA cycle activity enhancement in premature babies. A derangement in energy metabolism is further supported by the changes in ketone bodies (↓ 3-HBA and acetone), ketogenic amino acid lysine (↑, but possibly also gender-related), 4-DTA (↓, a product of threonine catabolism[52] and related to 3-HBA[53]), and lactate (↓) (Figure 6). Previous studies have associated prematurity with enhanced use of fatty acids as a source of energy at the time of birth[8] and the decreased ketone bodies suggest their higher consumption for TCA cycle enhancement in extra hepatic tissues, for energy production. The decrease in lactate is consistent with a possible enhanced use of pyruvate into the TCA cycle.

Variations in ethanolamine (↓) and *myo*-inositol (↑) may reflect changes in the synthesis of membrane phospholipids phosphatidylethanolamine and phosphatidylinositol (PI), which act as lung surfactants.[54] In this cohort, premature babies were born approximately at the gestational age characterized by enhanced PI formation (32−35 g.w.), just before its declining until the end of gestation. Therefore, increased urinary *myo*-inositol could reflect that temporary higher demand for PI synthesis. However, other reasons may be advanced for *myo*-inositol changes, namely a possible contribution from gender, a relation with renal function disturbance,[18] or an indication of insulin resistance, as noted for IUGR newborns.[21] A possible relation to renal function is supported by other indicators namely, the lower levels of

DOI: 10.1021/acs.jproteome.5b00977
J. Proteome Res. XXXX, XXX, XXX−XXX

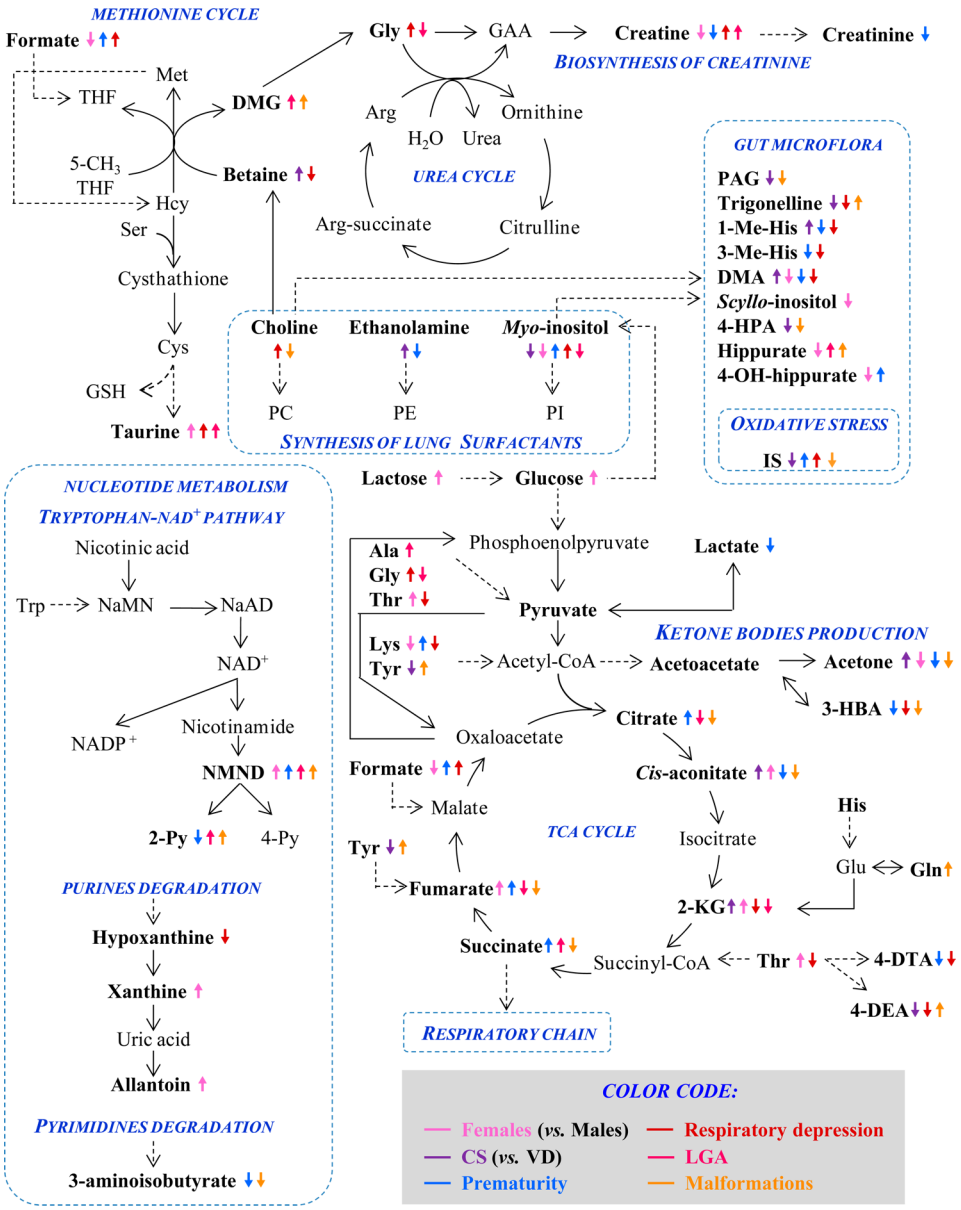

Figure 6. Schematic representation of the main metabolic pathways affected due to gender and delivery mode and in cases of prematurity, respiratory depression, LGA newborns and malformations, seen through newborn urine (changes noted correspond to those listed in Tables 2 and 3). Metabolites in bold are those observed by NMR. Color code: light pink: females (vs males), purple: CS (vs VD), blue: prematurity, red: respiratory depression, deep pink: LGA, orange: malformations. Amino acids in 3-letter code; NaMN: nicotinic acid mono nucleotide, NaAD: nicotinic acid adenine dinucleotide, NAD+: nicotinamide adenine dinucleotide, NADP: nicotinamide dinucleotide phosphate, ADP: adenosine diphosphate, NMND: *N*-methyl-nicotinamide, 2-Py: *N*-methyl-2-pyridone-5-carboxamide, 4-Py: *N*-methyl-4-pyridone-3-carboxamide, 4-DEA: 4-deoxyerythronic acid, 4-DTA: 4-deoxythreonic acid, 3-HBA: 3-hydroxybutyrate, PAG: phenylacetylglutamine, DMA: dimethylamine, PI: phosphatidylinositol, PE: phosphatidylethanolamine, PC: phopshatidylcholine, DMG: dimethylglycine, GAA: guanidoacetate, Hcy: homocysteine, GSH: gluthathione, THF: tetrahydrofolate.

creatinine, previously associated with immature tubular and vascular structures in the kidney,[55] and of methylguanidine, an uremic toxin formed from creatinine via creatol,[56] although with a possible gender contribution. The higher IS levels in premature newborns may be reflective of increased oxidative stress[57] but increased IS in urine and serum of adults has also been interpreted as reflective of impaired renal function.[58,59] Other significant changes related to prematurity include 3-hydroxyisovalerate (3-HIVA) (↑), DMA (↓) and 1-methylhistidine (↓), the latter two compounds being related with gut microflora and the former having been proposed as a marker of reduced biotin status.[60]

Comparison of the above observations with groups of term newborns suffering from other abnormal conditions unveiled that, not only prematurity seems to be characterized by a specific urinary signature, but also that newborns affected by respiratory depression episode, LGA or malformations also evidence their own specific metabolic signatures. This indicates that NMR metabolomics of newborn urine is capable of distinguishing different conditions, in addition to detecting general metabolic disturbances dues to generalized stress effects. Accordingly, the urinary signatures found for respiratory depression, LGA, and malformations are also putatively interpreted below. In relation to the newborns affected by a

DOI: 10.1021/acs.jproteome.5b00977
J. Proteome Res. XXXX, XXX, XXX−XXX

respiratory depression episode at birth (depressed Apgar score in the first minute, but without other clinical signs of asphyxia), a parallelism with neonatal asphyxia may be drawn to some extent, bearing in mind that the latter implies a more severe case of oxygen deprivation and comprises other sequelae. Variations in glycine (↑), betaine (↑), taurine (↑), creatine (↑), *myo*-inositol (↑) and 4-DEA (↓) were found to have the highest statistical significance (Figure 6, red arrows). Increased glycine, an excitatory neurotransmitter, has been reported in cerebral spinal fluid (CSF) of neonates with asphyxia and HIE,[61] being suggested that perinatal asphyxia enhances glycine prouction. The concomitant alterations in betaine, choline, creatine and taurine are consistent with perturbation of the methionine cycle. Regarding *myo*-inositol, high levels in the brain of HIE newborns have been reported,[62] this having been related to gliosis (proliferation of astrocytes after central nervous system, CNS, injury) and poor myelination.[62] In addition, the function of *myo*-inositol as precursor of lung surfactant PI may also be important in relation to the development of the respiratory depression episode. In the LGA cohort, varying urine metabolites include *myo*-inositol (↓), DMG (↑) and 2-Py (↑) (Figure 6, dark pink arrows). Higher *myo*-inositol levels have been noted in the urine of IUGR and LGA newborns and suggested to reflect altered glucose metabolism.[22] Our observation of less *myo*-inositol in LGA babies contradicts previous observations, while suggesting that other effects may contribute to *myo*-inositol levels, for example, alterations in lung surfactant metabolism. The higher urinary DMG and 2-Py levels may originate from changes in methionine cycle and nucleotides metabolism, respectively (Figure 6). Increased DMG has been correlated with higher birth weight, in a LBW vs normal weight cohort, due to alterations in choline metabolism.[63] Moreover, it has been suggested that alterations in methionine metabolism could impact on purine and pyrimidine metabolism, deoxyribonucleic acid (DNA) synthesis and/or cell proliferation, and affect fetal growth.[64] This is consistent with the noted disturbances in the tryptophan-nicotinamide adenine dinucleotide (tryptophan-NAD^+) pathway (Figure 6) and the significant intensity decrease of purines/pyrimidines resonances at δ 6.0−6.5. Notably, the bile acids region (δ 0.5−1.0)[19] is significantly increased in LGA newborns, but no explanations for this may be advanced at this stage. Finally, the heterogeneous malformations group seems to evidence general effects on succinate (↓), IS (↓), citrate (↓), and 2-Py (↓) (Figure 6, orange arrows). A lower level of succinate has also been observed in maternal urine of women carrying malformed fetuses,[32] possibly reflecting its underuse in the respiratory chain and/or as an intermediate of the TCA cycle, along with citrate, *cis*-aconitate and fumarate, all decreased in this cohort (Figure 6). IS has been seen to increase in the maternal urine of CNS malformations cases, due to increased oxidative stress,[32] however, in this cohort it may also carry a reflection of delivery mode. Nucleotide metabolism, particularly the tryptophan-NAD^+ pathway, also seems to be altered in cases of malformations, as shown by 2-Py and NMND levels (Figure 6), the latter having been noted in the urine of women carrying malformed fetuses.[32] It is interesting to note that, although generally distinct signatures are observed for the four different conditions studied (Figure 6), the increase in NMND and the decrease in 3-HBA seem to occur consistently (in at least three of the disorders), thus suggesting that general stress effects impact on nucleotide metabolism and ketone body production.

CONCLUSIONS

This paper reports a comprehensive NMR metabolomics study of newborn urine to study the metabolic impact of prematurity, compared to other newborn disorders (namely respiratory depression episode, large for gestational age and malformations) and taking into account important confounders. First, results have shown that gender and delivery mode have significant impacts on urine composition and, hence, need to be considered when subject groups are unmatched in these respects. Subsequently, premature newborns were found to be characterized by a wide signature of varying metabolites, indicative of disturbances in nucleotide metabolism, lung surfactants biosynthesis, and renal function, along with enhancement of TCA cycle activity, fatty acids oxidation and oxidative stress. This signature was substantially distinct from those characterizing other disorders, since (1) newborns who suffered a respiratory depression episode revealed increased glycine excretion (possibly reflecting alterations in cerebral synthesis of neurotransmitters), alterations in methionine cycle and *myo*-inositol (possibly due to mild indication of possible brain insult and/or lung surfactant biosynthesis alterations), (2) LGA newborns showed *myo*-inositol changes (possibly indicative of altered glucose handling and/or lung surfactant metabolism), changes in methionine cycle and purines/pyrimidines metabolism, with a suggestion of some role played by bile acids, (3) the small heterogeneous group of malformations seemed to share a TCA cycle slowing down and a disturbance of nucleotides metabolism. Interestingly, in addition to the observed signature differences, changes in NMND and 3-HBA seems to reflect general metabolic effects (nucleotide metabolism and ketone body synthesis) present in most of the disorders studied.

This work shows that NMR metabolomics is successful in extracting detailed and largely specific information on the urine composition of newborns affected by several disorders. The putative biochemical interpretations advanced here require future biological demonstration and validation in large cohorts, in order to lay the ground for the clinical use of specific metabolic signatures as diagnostic and prognostic markers. Regarding prematurity, in particular, this knowledge may become useful to (1) assess the extent of the specific consequences of the condition on each newborn, (2) correlate to possible prenatal biomarkers found in maternal biofluids and which may be predictive of prematurity, and (3) identify and distinguish short- and long-term effects of prematurity.

ASSOCIATED CONTENT

Supporting Information

The Supporting Information is available free of charge on the ACS Publications website at DOI: 10.1021/acs.jproteome.5b00977.

Figure S1. Q^2 distributions (left) and ROC maps (right) of true and permuted models obtained for the ^{1}H NMR spectra of newborn urine after variable selection of a) female n = 23 vs male n = 23 and b) prematurity n = 17 vs controls n = 46. Q^2: predictive power; TPR: true positive rate; FPR: false positive rate. Figure S2. VIP-wheel representation of the NMR metabolite signatures (left) and Volcano plots of effect size vs−log(p-value) of the metabolite/resonances integrals listed in Table 2 (right) obtained for (a) gender (female vs male newborns) and for (b) delivery mode (CS vs VD).

DOI: 10.1021/acs.jproteome.5b00977
J. Proteome Res. XXXX, XXX, XXX−XXX

Colored shade in VIP-wheel representation indicates region typically containing resonances of bile acids (green), aliphatic region (blue), sugar region (pink) and aromatic region (orange). Metabolites or spectral regions with higher VIP values are noted. *: spectral features corresponding to large VIP values but with no statistical relevance (p value >0.05). Figure S3. PLS-DA scores scatter plot obtained for prematurity (blue circles, n = 17) compared to controls (black circles, n = 46), where symbol diameter represents (a) gestational age at birth and (b) birth weight. Table S1. Peak assignments in the ^{1}H NMR spectra of newborn urine, at pH 7.00 ± 0.02. s: singlet, d: doublet, t: triplet, q: quartet, dd: doublet of doublets, m: multiplet. [a] Indicates compounds identified in newborn urine for the first time to our knowledge, compared to literature. Table S2. Q^2 (predictive power) values and MCCV parameters obtained for the PLS-DA models corresponding to (a) full resolution data sets and (b) data sets obtained after variable selection. GA: gestational age, CR: classification rate, Sens.: sensitivity, Spec.: specificity, Q^2: cumulative predictive power obtained by cross-validation, Q^2_m: median Q^2 obtained by MCCV. * Models not considered robust principally due to poor ROC maps and/or poor quality of Q^2distributions (PDF)

AUTHOR INFORMATION

Corresponding Author

*Tel: +351 234 370707. Fax: +351 234 370084. E-mail: agil@ua.pt.

Author Contributions

S.O.D. and J.P. contributed equally.

S.D. carried out the NMR analysis of urine samples, the spectral data analysis and drafted part of the manuscript. J.P. improved on all tables and graphics, drafted and updated part of the manuscript. E.M. helped with data acquisition and preliminary data analysis and D.D. helped in metadata collection and organization. F.M., C.P., M.C.A., and I.M.C. helped to define the design and setting up of sampling protocols, subject guidance and information on the project, as well as in the biochemical interpretation of results. A.S.B. helped in the variable selection work, definition of graphics and data analysis interpretation. M.S. aided in the data interpretation and access to spectral databases. A.M.G. conceived the study, participated in its design and coordination and finalised the writing of the manuscript. All authors read and approved the final manuscript. S.O.D. and J.P. contributed equally to this work.

Notes

The authors declare no competing financial interest.

ACKNOWLEDGMENTS

This work was developed within the scope of the project CICECO-Aveiro Institute of Materials (FCT UID/CTM/50011/2013), financed by national funds through the FCT/MEC and cofinanced by FEDER under the PT2020 Partnership Agreement and QOPNA FCT-Funding: PEst-C/QUI/UI0062/2013. S.D. thanks FCT for the SFRH/BD/64159/2009 grant. JP thanks FCT for the SFRH/BD/73343/2010 and Bruker BioSpin grants. D.D. acknowledges funds from the Observatoire Hommes-Milieux International (OHM.I) "Estarreja" (OHM-E/2014/Proj.1). We acknowledge the Portuguese National NMR Network (RNRMN), supported by FCT funds.

REFERENCES

(1) Mussap, M.; Antonucci, R.; Noto, A.; Fanos, V. The role of metabolomics in neonatal and pediatric laboratory medicine. *Clin. Chim. Acta* **2013**, *426*, 127−138.

(2) Pinto, J.; Domingues, M. R.; Gil, A. M. Blood metabolomics in human prenatal and newborn health studies. In *Global Metabolic Profiling: Clinical Applications*; Nichols, A., Theodoridis, G., Wilson, I. D., Eds.; Future Science Ltd: London, 2014; pp 50−68.

(3) Peng, S.; Zhang, J.; Liu, L.; Zhang, X.; Huang, Q.; Alamdar, A.; Tian, M.; Shen, H. Newborn Meconium and Urinary Metabolome Response to Maternal Gestational Diabetes Mellitus: A Preliminary Case-Control Study. *J. Proteome Res.* **2015**, *14*, 1799−1809.

(4) Horgan, R. P.; Broadhurst, D. I.; Walsh, S. K.; Dunn, W. B.; Brown, M.; Roberts, C. T.; North, R. A.; McCowan, L. M.; Kell, D. B.; Baker, P. N.; et al. Metabolic Profiling Uncovers a Phenotypic Signature of Small for Gestational Age in Early Pregnancy. *J. Proteome Res.* **2011**, *10*, 3660−3673.

(5) Favretto, D.; Cosmi, E.; Ragazzi, E.; Visentin, S.; Tucci, M.; Fais, P.; Cecchetto, G.; Zanardo, V.; Viel, G.; Ferrara, S. D. Cord blood metabolomic profiling in intrauterine growth restriction. *Anal. Bioanal. Chem.* **2012**, *402*, 1109−1121.

(6) Sanz-Cortés, M.; Carbajo, R. J.; Crispi, F.; Figueras, F.; Pineda-Lucena, A.; Gratacós, E. Metabolomic profile of umbilical cord blood plasma from early and late intrauterine growth restricted (IUGR) neonates with and without signs of brain vasodilation. *PLoS One* **2013**, *8*, e80121.

(7) Ivorra, C.; Garcia-Vicent, C.; Chaves, F. J.; Monleon, D.; Manuel Morales, J.; Lurbe, E. Metabolomic profiling in blood from umbilical cords of low birth weight newborns. *J. Transl. Med.* **2012**, *10*, 1−10.

(8) Alexandre-Gouabau, M.-C.; Courant, F.; Moyon, T.; Küster, A.; Le Gall, G.; Tea, I.; Antignac, J.-P.; Darmaun, D. Maternal and cord blood LC-HRMS metabolomics reveal alterations in energy and polyamine metabolism, and oxidative stress in very-low birth weight infants. *J. Proteome Res.* **2013**, *12*, 2764−2778.

(9) Walsh, B. H.; Broadhurst, D. I.; Mandal, R.; Wishart, D. S.; Boylan, G. B.; Kenny, L. C.; Murray, D. M. The Metabolomic Profile of Umbilical Cord Blood in Neonatal Hypoxic Ischaemic Encephalopathy. *PLoS One* **2012**, *7*, e50520.

(10) Reinke, S. N.; Walsh, B. H.; Boylan, G. B.; Sykes, B. D.; Kenny, L. C.; Murray, D. M.; Broadhurst, D. I. ^{1}H NMR derived metabolomic profile of neonatal asphyxia in umbilical cord serum: implications for hypoxic ischemic encephalopathy. *J. Proteome Res.* **2013**, *12*, 4230−4239.

(11) Longini, M.; Giglio, S.; Perrone, S.; Vivi, A.; Tassini, M.; Fanos, V.; Sarafidis, K.; Buonocore, G. Proton nuclear magnetic resonance spectroscopy of urine samples in preterm asphyctic newborn: A metabolomic approach. *Clin. Chim. Acta* **2015**, *444*, 250−256.

(12) Dani, C.; Bresci, C.; Berti, E.; Ottanelli, S.; Mello, G.; Mecacci, F.; Breschi, R.; Hu, X.; Tenori, L.; Luchinat, C. Metabolomic profile of term infants of gestational diabetic mothers. *J. Matern.-Fetal Neonat. Med.* **2014**, *27*, 537−542.

(13) Hashimoto, F.; Nishiumi, S.; Miyake, O.; Takeichi, H.; Chitose, M.; Ohtsubo, H.; Ishimori, S.; Ninchoji, T.; Hashimura, Y.; Kaito, H.; et al. Metabolomics analysis of umbilical cord blood clarifies changes in saccharides associated with delivery method. *Early Hum. Dev.* **2013**, *89*, 315−320.

(14) Constantinou, M.; Papakonstantinou, E.; Benaki, D.; Spraul, M.; Shulpis, K.; Koupparis, M.; Mikros, E. Application of nuclear magnetic resonance spectroscopy combined with principal component analysis in detecting inborn errors of metabolism using blood spots: a metabonomic approach. *Anal. Chim. Acta* **2004**, *511*, 303−312.

(15) Dénes, J.; Szabo, E.; Robinette, S. L.; Szatmari, I.; Szonyi, L.; Kreuder, J. G.; Rauterberg, E. W.; Takats, Z. Metabonomics of Newborn Screening Dried Blood Spot Samples: A Novel Approach in the Screening and Diagnostics of Inborn Errors of Metabolism. *Anal. Chem.* **2012**, *84*, 10113−10120.

DOI: 10.1021/acs.jproteome.5b00977
J. Proteome Res. XXXX, XXX, XXX−XXX

(16) Sahoo, S.; Franzson, L.; Jonsson, J. J.; Thiele, I. A compendium of inborn errors of metabolism mapped onto the human metabolic network. *Mol. BioSyst.* **2012**, *8*, 2545−2558.
(17) Brown, J. C. C.; Mills, G. A.; Sadler, P. J.; Walker, V. ^{1}H NMR studies of urine from premature and sick babies. *Magn. Reson. Med.* **1989**, *11*, 193−201.
(18) Foxall, P. J.; Bewley, S.; Neild, G. H.; Rodeck, C. H.; Nicholson, J. K. Analysis of fetal and neonatal urine using proton nuclear magnetic resonance spectroscopy. *Arch. Dis. Child. Fetal Neonatal Ed.* **1995**, *73*, F153−F157.
(19) Trump, S.; Laudi, S.; Unruh, N.; Goelz, R.; Leibfritz, D. ^{1}H-NMR metabolic profiling of human neonatal urine. *MAGMA* **2007**, *19*, 305−312.
(20) Atzori, L.; Antonucci, R.; Barberini, L.; Locci, E.; Marincola, F. C.; Scano, P.; Cortesi, P.; Agostiniani, R.; Defraia, R.; Weljie, A.; et al. ^{1}H NMR-based metabolomic analysis of urine from preterm and term neonates. *Front. Biosci., Elite Ed.* **2011**, *3*, 1005−1012.
(21) Dessì, A.; Atzori, L.; Noto, A.; Visser, G. H. A.; Gazzolo, D.; Zanardo, V.; Barberini, L.; Puddu, M.; Ottonello, G.; Atzei, A.; et al. Metabolomics in newborns with intrauterine growth retardation (IUGR): urine reveals markers of metabolic syndrome. *J. Matern.-Fetal Neonat. Med.* **2011**, *24* (Suppl 2), 35−39.
(22) Dessì, A.; Marincola, F. C.; Pattumelli, M. G.; Ciccarelli, S.; Corbu, S.; Ossicini, C.; Fanos, V.; Agostino, R. Investigation of the ^{1}H-NMR based urine metabolomic profiles of IUGR, LGA and AGA newborns on the first day of life. *J. Matern.-Fetal Neonat. Med.* **2014**, *27* (Suppl 2), 13−19.
(23) Barberini, L.; Noto, A.; Fattuoni, C.; Grapov, D.; Casanova, A.; Fenu, G.; Gaviano, M.; Carboni, R.; Ottonello, G.; Crisafulli, M.; et al. Urinary metabolomics (GC-MS) reveals that low and high birth weight infants share elevated inositol concentrations at birth. *J. Matern.-Fetal Neonat. Med.* **2014**, *27* (Suppl 2), 20−26.
(24) Ma, S.; Shieh, L. I.; Huang, C. C. High-resolution proton nuclear magnetic resonance studies of urine from asphyxiated newborn infants. *Appl. Biochem. Biotechnol.* **1995**, *53*, 37−51.
(25) Chu, C. Y.; Xiao, X.; Zhou, X. G.; Lau, T. K.; Rogers, M. S.; Fok, T. F.; Law, L. K.; Pang, C. P.; Wang, C. C. Metabolomic and bioinformatic analyses in asphyxiated neonates. *Clin. Biochem.* **2006**, *39*, 203−209.
(26) Fanos, V.; Pintus, M. C.; Lussu, M.; Atzori, L.; Noto, A.; Stronati, M.; Guimaraes, H.; Marcialis, M. A.; Rocha, G.; Moretti, C.; et al. Urinary metabolomics of bronchopulmonary dysplasia (BPD): preliminary data at birth suggest it is a congenital disease. *J. Matern.-Fetal Neonat. Med.* **2014**, *27* (Suppl2), 39−45.
(27) Constantinou, M. A.; Papakonstantinou, E.; Spraul, M.; Sevastiadou, S.; Costalos, C.; Koupparis, M. A.; Shulpis, K.; Tsantili-Kakoulidou, A.; Mikros, E. ^{1}H NMR-based metabonomics for the diagnosis of inborn errors of metabolism in urine. *Anal. Chim. Acta* **2005**, *542*, 169−177.
(28) Fanos, V.; Caboni, P.; Corsello, G.; Stronati, M.; Gazzolo, D.; Noto, A.; Lussu, M.; Dessì, A.; Giuffrè, M.; Lacerenza, S.; et al. Urinary ^{1}H-NMR and GC-MS metabolomics predicts early and late onset neonatal sepsis. *Early Hum. Dev.* **2014**, *90* (Suppl 1), S78−S83.
(29) Fanos, V.; Locci, E.; Noto, A.; Lazzarotto, T.; Manzoni, P.; Atzori, L.; Lanari, M. Urinary metabolomics in newborns infected by human cytomegalovirus: a preliminary investigation. *Early Hum. Dev.* **2013**, *89* (Suppl 1), S58−S61.
(30) Dessì, A.; Liori, B.; Caboni, P.; Corsello, G.; Giuffrè, M.; Noto, A.; Serraino, F.; Stronati, M.; Zaffanello, M.; Fanos, V. Monitoring neonatal fungal infection with metabolomics. *J. Matern.-Fetal Neonat. Med.* **2014**, *27* (Suppl2), 34−38.
(31) Dessì, A.; Ottonello, G.; Fanos, V. Physiopathology of intrauterine growth retardation: from classic data to metabolomics. *J. Matern.-Fetal Neonat. Med.* **2012**, *25*, 13−18.
(32) Diaz, S. O.; Barros, A. S.; Goodfellow, B. J.; Duarte, I. F.; Galhano, E.; Pita, C.; Almeida, M. do C.; Carreira, I. M.; Gil, A. M. Second trimester maternal urine for the diagnosis of trisomy 21 and prediction of poor pregnancy outcomes. *J. Proteome Res.* **2013**, *12*, 2946−2957.
(33) Wishart, D. S.; Knox, C.; Guo, A. C.; Eisner, R.; Young, N.; Gautam, B.; Hau, D. D.; Psychogios, N.; Dong, E.; Bouatra, S.; et al. HMDB: a knowledgebase for the human metabolome. *Nucleic Acids Res.* **2009**, *37*, D603−D610.
(34) Cloarec, O.; Dumas, M.-E.; Craig, A.; Barton, R. H.; Trygg, J.; Hudson, J.; Blancher, C.; Gauguier, D.; Lindon, J. C.; Holmes, E.; et al. Statistical Total Correlation Spectroscopy: An Exploratory Approach for Latent Biomarker Identification from Metabolic ^{1}H NMR Data Sets. *Anal. Chem.* **2005**, *77*, 1282−1289.
(35) Veselkov, K. A.; Lindon, J. C.; Ebbels, T. M. D.; Crockford, D.; Volynkin, V. V.; Holmes, E.; Davies, D. B.; Nicholson, J. K. Recursive segment-wise peak alignment of biological ^{1}H NMR spectra for improved metabolic biomarker recovery. *Anal. Chem.* **2009**, *81*, 56−66.
(36) Dieterle, F.; Ross, A.; Schlotterbeck, G.; Senn, H. Probabilistic quotient normalization as robust method to account for dilution of complex biological mixtures. Application in ^{1}H NMR metabonomics. *Anal. Chem.* **2006**, *78*, 4281−4290.
(37) Wiklund, S.; Nilsson, D.; Eriksson, L.; Sjöström, M.; Wold, S.; Faber, K. A randomization test for PLS component selection. *J. Chemom.* **2007**, *21*, 427−439.
(38) Westerhuis, J. A.; Hoefsloot, H. C. J.; Smit, S.; Vis, D. J.; Smilde, A. K.; van Velzen, E.; van Duijnhoven, J.; van Dorsten, F.; Velzen, E. J. J.; Duijnhoven, J. P. M.; et al. Assessment of PLSDA cross validation. *Metabolomics* **2008**, *4*, 81−89.
(39) Berben, L.; Sereika, S. M.; Engberg, S. Effect size estimation: methods and examples. *Int. J. Nurs. Stud.* **2012**, *49*, 1039−1047.
(40) Benjamini, Y.; Hochberg, Y. Controlling the false discovery rate: a practical and powerful approach to multiple testing. *J. R. Stat. Soc. Ser. B* **1995**, *57*, 289−300.
(41) Kochhar, S.; Jacobs, D. M.; Ramadan, Z.; Berruex, F.; Fuerholz, A.; Fay, L. B. Probing gender-specific metabolism differences in humans by nuclear magnetic resonance-based metabonomics. *Anal. Biochem.* **2006**, *352*, 274−281.
(42) Slupsky, C. M.; Rankin, K. N.; Wagner, J.; Fu, H.; Chang, D.; Weljie, A. M.; Saude, E. J.; Lix, B.; Adamko, D. J.; Shah, S.; et al. Investigations of the effects of gender, diurnal variation, and age in human urinary metabolomic profiles. *Anal. Chem.* **2007**, *79*, 6995−7004.
(43) Psihogios, N. G.; Gazi, I. F.; Elisaf, M. S.; Seferiadis, K. I.; Bairaktari, E. T. Gender-related and age-related urinalysis of healthy subjects by NMR-based metabonomics. *NMR Biomed.* **2008**, *21*, 195−207.
(44) Ramautar, R.; Nevedomskaya, E.; Mayboroda, O. A.; Deelder, A. M.; Wilson, I. D.; Gika, H. G.; Theodoridis, G. A.; Somsen, G. W.; de Jong, G. J. Metabolic profiling of human urine by CE-MS using a positively charged capillary coating and comparison with UPLC-MS. *Mol. BioSyst.* **2011**, *7*, 194−199.
(45) Croze, M. L.; Soulage, C. O. Potential role and therapeutic interests of myo-inositol in metabolic diseases. *Biochimie* **2013**, *95*, 1811−1827.
(46) Morelli, L. Postnatal Development of Intestinal Microflora as Influenced by Infant Nutrition. *J. Nutr.* **2008**, *138*, 1791S−1795.
(47) Vakilian, K.; Ranjbar, A.; Zarganjfard, A.; Mortazavi, M.; Vosough-Ghanbari, S.; Mashaiee, S.; Abdollahi, M. On the relation of oxidative stress in delivery mode in pregnant women; a toxicological concern. *Toxicol. Mech. Methods* **2009**, *19*, 94−99.
(48) Hyde, M. J.; Griffin, J. L.; Herrera, E.; Byrne, C. D.; Clarke, L.; Kemp, P. R. Delivery by Caesarean section, rather than vaginal delivery, promotes hepatic steatosis in piglets. *Clin. Sci.* **2010**, *118*, 47−59.
(49) Watanabe, K.; Iwasaki, A.; Mori, T.; Kimura, C.; Matsushita, H.; Shinohara, K.; Wakatsuki, A. Differences in levels of oxidative stress in mothers and neonate: the impact of mode of delivery. *J. Matern.-Fetal Neonat. Med.* **2013**, *26*, 1649−1652.
(50) Dou, L.; Jourde-Chiche, N.; Faure, V.; Cerini, C.; Berland, Y.; Dignat-George, F.; Brunet, P. The uremic solute indoxyl sulfate induces oxidative stress in endothelial cells. *J. Thromb. Haemostasis* **2007**, *5*, 1302−1308.

DOI: 10.1021/acs.jproteome.5b00977
J. Proteome Res. XXXX, XXX, XXX−XXX

(51) Lamarre, S. G.; Morrow, G.; Macmillan, L.; Brosnan, M. E.; Brosnan, J. T. Formate: an essential metabolite, a biomarker, or more? *Clin. Chem. Lab. Med.* **2013**, *51*, 571−578.
(52) Appiah-Amponsah, E.; Shanaiah, N.; Nagana Gowda, G. A.; Owusu-Sarfo, K.; Ye, T.; Raftery, D. Identification of 4-deoxythreonic acid present in human urine using HPLC and NMR techniques. *J. Pharm. Biomed. Anal.* **2009**, *50*, 878−885.
(53) Diaz, S. O.; Barros, A. S.; Goodfellow, B. J.; Duarte, I. F.; Carreira, I. M.; Galhano, E.; Pita, C.; Almeida, M. do C.; Gil, A. M. Following healthy pregnancy by nuclear magnetic resonance (NMR) metabolic profiling of human urine. *J. Proteome Res.* **2013**, *12*, 969−979.
(54) Agassandian, M.; Mallampalli, R. K. Surfactant phospholipid metabolism. *Biochim. Biophys. Acta, Mol. Cell Biol. Lipids* **2013**, *1831*, 612−625.
(55) Lage, S.; Andrade, F.; Prieto, J. A.; Asla, I.; Rodríguez, A.; Ruiz, N.; Echeverría, J.; Luz Couce, M.; Sanjurjo, P.; Aldámiz-Echevarría, L. Arginine-guanidinoacetate-creatine pathway in preterm newborns: creatine biosynthesis in newborns. *J. Pediatr. Endocrinol. Metab.* **2013**, *26*, 53−60.
(56) Marescau, B.; Nagels, G.; Possemiers, I.; De Broe, M. E.; Becaus, I.; Billiouw, J.-M.; Lornoy, W.; De Deyn, P. P. Guanidino compounds in serum and urine of nondialyzed patients with chronic renal insufficiency. *Metab., Clin. Exp.* **1997**, *46*, 1024−1031.
(57) Perrone, S.; Mussap, M.; Longini, M.; Fanos, V.; Bellieni, C. V.; Proietti, F.; Cataldi, L.; Buonocore, G. Oxidative kidney damage in preterm newborns during perinatal period. *Clin. Biochem.* **2007**, *40*, 656−660.
(58) Suhre, K.; Meisinger, C.; Döring, A.; Altmaier, E.; Belcredi, P.; Gieger, C.; Chang, D.; Milburn, M. V.; Gall, W. E.; Weinberger, K. M.; et al. Metabolic footprint of diabetes: a multiplatform metabolomics study in an epidemiological setting. *PLoS One* **2010**, *5*, e13953.
(59) Huang, S.-T.; Shu, K.-H.; Cheng, C.-H.; Wu, M.-J.; Yu, T.-M.; Chuang, Y.-W.; Chen, C.-H. Serum total p-cresol and indoxyl sulfate correlated with stage of chronic kidney disease in renal transplant recipients. *Transplant. Proc.* **2012**, *44*, 621−624.
(60) Bahado-Singh, R. O.; Akolekar, R.; Mandal, R.; Dong, E.; Xia, J.; Kruger, M.; Wishart, D. S.; Nicolaides, K. Metabolomic analysis for first-trimester Down syndrome prediction. *Am. J. Obstet. Gynecol.* **2013**, *208*, 371.e1−371.e8.
(61) Roldán, A.; Figueras-Aloy, J.; Deulofeu, R.; Jiménez, R. Glycine and other neurotransmitter amino acids in cerebrospinal fluid in perinatal asphyxia and neonatal hypoxic-ischaemic encephalopathy. *Acta Paediatr.* **1999**, *88*, 1137−1141.
(62) Fan, G.; Wu, Z.; Chen, L.; Guo, Q.; Ye, B.; Mao, J. Hypoxia-ischemic encephalopathy in full-term neonate: correlation proton MR spectroscopy with MR imaging. *Eur. J. Radiol.* **2003**, *45*, 91−98.
(63) Hogeveen, M.; den Heijer, M.; Semmekrot, B. A.; Sporken, J. M.; Ueland, P. M.; Blom, H. J. Umbilical choline and related methylamines betaine and dimethylglycine in relation to birth weight. *Pediatr. Res.* **2013**, *73*, 783−787.
(64) Kalhan, S. C.; Marczewski, S. E. Methionine, homocysteine, one carbon metabolism and fetal growth. *Rev. Endocr. Metab. Disord.* **2012**, *13*, 109−119.

DOI: 10.1021/acs.jproteome.5b00977
J. Proteome Res. XXXX, XXX, XXX−XXX